

We are IntechOpen, the world's leading publisher of Open Access books Built by scientists, for scientists

6,900

Open access books available

186,000

International authors and editors

200M

Downloads

Our authors are among the

154

Countries delivered to

TOP 1%

most cited scientists

12.2%

Contributors from top 500 universities



WEB OF SCIENCE™

Selection of our books indexed in the Book Citation Index
in Web of Science™ Core Collection (BKCI)

Interested in publishing with us?
Contact book.department@intechopen.com

Numbers displayed above are based on latest data collected.
For more information visit www.intechopen.com



Twin Deformation Mechanisms in Nanocrystalline and Ultrafine-Grained Materials

Nikolay Skiba

Additional information is available at the end of the chapter

<http://dx.doi.org/10.5772/intechopen.74978>

Abstract

The review of the theoretical models, which describes mechanisms of deformation twinning in nanocrystalline and ultrafine-grained materials, is presented. Realization of special mechanisms of nanoscale deformation twin generation at locally distorted grain boundaries (GBs) in nanocrystalline and ultrafine-grained materials is observed. In particular, the micromechanisms of deformation twin formation occur through (1) the consequent emission of partial dislocations from GBs; (2) the cooperative emission of partial dislocations from GBs; and (3) the generation of multiplane nanoscale shear at GBs. The energy and stress characteristics of the deformation nanotwin generation at GBs in nanocrystalline and ultrafine-grained materials are calculated and analyzed. Competition between the twin generation mechanisms in nanocrystalline and ultrafine-grained materials is discussed.

Keywords: nanocrystalline and ultrafine-grained materials, nanotwins, plastic deformation, grain boundaries, dislocations

1. Introduction

At present, the study of the plastic behavior of nanostructured solids is one of the most important and rapidly developing directions in the mechanics of deformed solid and in the physics of condensed state. Nanostructured solids have unique physical, mechanical and chemical properties and are of great interest, both for fundamental and applied research [1]. For example, the strength and hardness of nanostructured materials are several times higher than those of conventional coarse-grained analogues of the same chemical composition. However, most nanocrystalline materials show low tensile ductility, which are highly undesirable for their practical applications. Increasing the ductility and fracture toughness of nanomaterials is a

very important task, the solution of which can significantly expand the field of their application. With a large volume fraction occupied by GBs which act as effective obstacles for lattice dislocation slip (the dominant deformation mechanism in conventional coarse-grained polycrystals), the conventional lattice dislocation slip is hampered in nanostructured materials. At the same time, the specific features of the structure of nanocrystalline materials provide the action of specific deformation mechanisms, and the effect of which in coarse-grained materials was not observed or was insignificant. Identification of these specific mechanisms of plastic deformation is a key problem for understanding the nature of ductility and fracture toughness of nanostructured solids. According to modern concepts of plastic flow processes, the following specific mechanisms of plastic deformation act in nanocrystalline and ultrafine-grained materials: GB sliding [2, 3], rotational deformation mode [4–6], GBs migration [7–9] and deformation twinning [10–13]. The analysis of experimental investigations of deformation mechanisms allows us to formulate the main difference between nanocrystalline materials exhibiting low and high ductility. The point is that each nanocrystalline sample consists of a number of structural elements: grains of different sizes, GBs of various types and misorientations. In this case, several mechanisms of plastic deformation can act simultaneously in a nanocrystalline sample under mechanical loading. In general, different mechanisms of plastic deformation dominate in neighboring grains of different sizes and adjacent GBs. In nanocrystalline materials with low ductility, different mechanisms of deformation act independently of each other, which lead to a substantial inhomogeneity of plastic deformation and can cause the nucleation and evolution of nanocracks. At the same time, in nanocrystalline materials exhibiting high ductility, different mechanisms of plastic deformation effectively interact with each other. Intensive crossovers occur between different deformation mechanisms which accommodate the inhomogeneities of plastic deformation. One of the main specific deformation modes which contribute greatly to plastic flow in nanocrystalline and ultrafine-grained materials is considered deformation twinning mechanism. Following numerous experimental data, computer simulations and theoretical models [10–17], nanoscale twin deformation effectively operates in nanomaterials with various chemical compositions and structures. In doing so, in contrast to coarse-grained polycrystals where deformation twins are typically generated within grain interiors, in nanomaterials under mechanical load, twins are often generated at GBs; see [12] and references therein. In order to explain this experimentally documented fact indicative of specific deformation behavior of nanomaterials, it was suggested that nanoscale deformation twinning occurs through consequent emission of partial dislocations from GBs [10–13]. However, in this situation, partial dislocations should exist on every slip plane or be transformed from pre-existent GB dislocations which is hardly possible in real materials [13]. In order to avoid the discussed discrepancy, Zhu and coworkers [13] suggested new micromechanism of partial dislocation multiplication which realized due to successive processes of dislocation reactions and cross-slips providing existence of the partial dislocations at a GB on every slip plane. Thus, further consequent emission of such partial dislocations from GB can provide a nanoscale formation at GB [13]. At the same time, this approach operates with dislocation reactions each transforming a partial dislocation into two dislocations: a full dislocation and another partial dislocation. Such reactions are specified by very large energy barriers (being around the energy of a full dislocation), and thereby they are hardly typical in real materials. In order to respond to these questions, in theoretical works [14, 15], alternative

mechanism of nanoscale twin formation at locally distorted GBs in deformed nanomaterials was suggested. According to results of the theoretical works [14, 15], GB dislocation can exist at locally distorted GB on every slip plane due to preceding plastic deformation and thereby cause nanoscale twin formation at GB. Taking this approach into account [14, 15], micromechanisms of deformation nanotwin formation can occur through (1) the consequent emission of partial dislocation from locally distorted GBs; (2) the cooperative emission of partial dislocations from locally distorted GBs; and (3) the generation of multiplane nanoscale shear at locally distorted GBs. Realization of these mechanisms is discussed in the next sections.

2. Mechanisms of deformation twin generation at locally distorted grain boundaries in nanocrystalline and ultrafine-grained materials

In this chapter, theoretical description of deformation twin generation mechanisms is based on results of the following theoretical papers [14–17]. According to these papers [14–17], generation of nanotwins occurs at locally distorted GB segments (GB segments being rich in GB dislocations) which were produced due to either events of consequent trapping of extrinsic lattice dislocations by GB and their splitting transformations into a wall of climbing GB dislocations (**Figure 1a–d**) or GB deformation processes involving slip and climb of GB dislocations (**Figure 1e–h**). The splitting of extrinsic dislocations at high-angle GBs is a well experimentally documented process [18] resulting at its initial stage in the formation of several closely located GB dislocations (**Figure 1a**). These processes allow GB dislocations to exist on almost every slip plane and thereby form a nanowall of GB dislocations (**Figure 1d**). In this situation, under action of external shear stress, a head dislocation of a pile-up is trapped by GB and splits into the GB dislocations (**Figure 1a** and **b**). After this process, the second lattice dislocation of the pile-up moves to and is trapped by GB where this dislocation splits into new GB dislocations (**Figure 1c**). In this case, after the splitting of the head dislocation of the pile-up, its second dislocation can reach the GB where this extrinsic dislocation splits into new GB dislocations (**Figure 1b** and **c**). Thus, consequent events of the splitting transformations of the head lattice dislocations forming pile-up into GB dislocations and climbing of these GB dislocations along GB can form a nanowall of GB dislocations located on almost every slip plane (**Figure 1d**). Both the transformation of GB dislocation into partial dislocations and emission of partial dislocation into grain interior are capable of producing a deformation nanotwin (for details, see below).

As follows from works [14, 15], formation of local distorted segments of GBs can be associated with GB plastic deformation processes. First, a nanostructured specimen is deformed by GB sliding that produces pile-ups of GB dislocations stopped by triple junctions of GBs (**Figure 1e**). Under the action of the external shear stress, the head GB dislocations of the pile-up split at triple junction and climb along GB (**Figure 1f–h**). As a result, a wall of climbing GB dislocations located on every (or almost every) slip plane is formed (**Figure 1h**). In general, local GB fragments being rich in GB dislocations can be formed at GBs “globally” distorted by plastic deformation. Such GBs are typical structural elements of bulk nanostructured materials

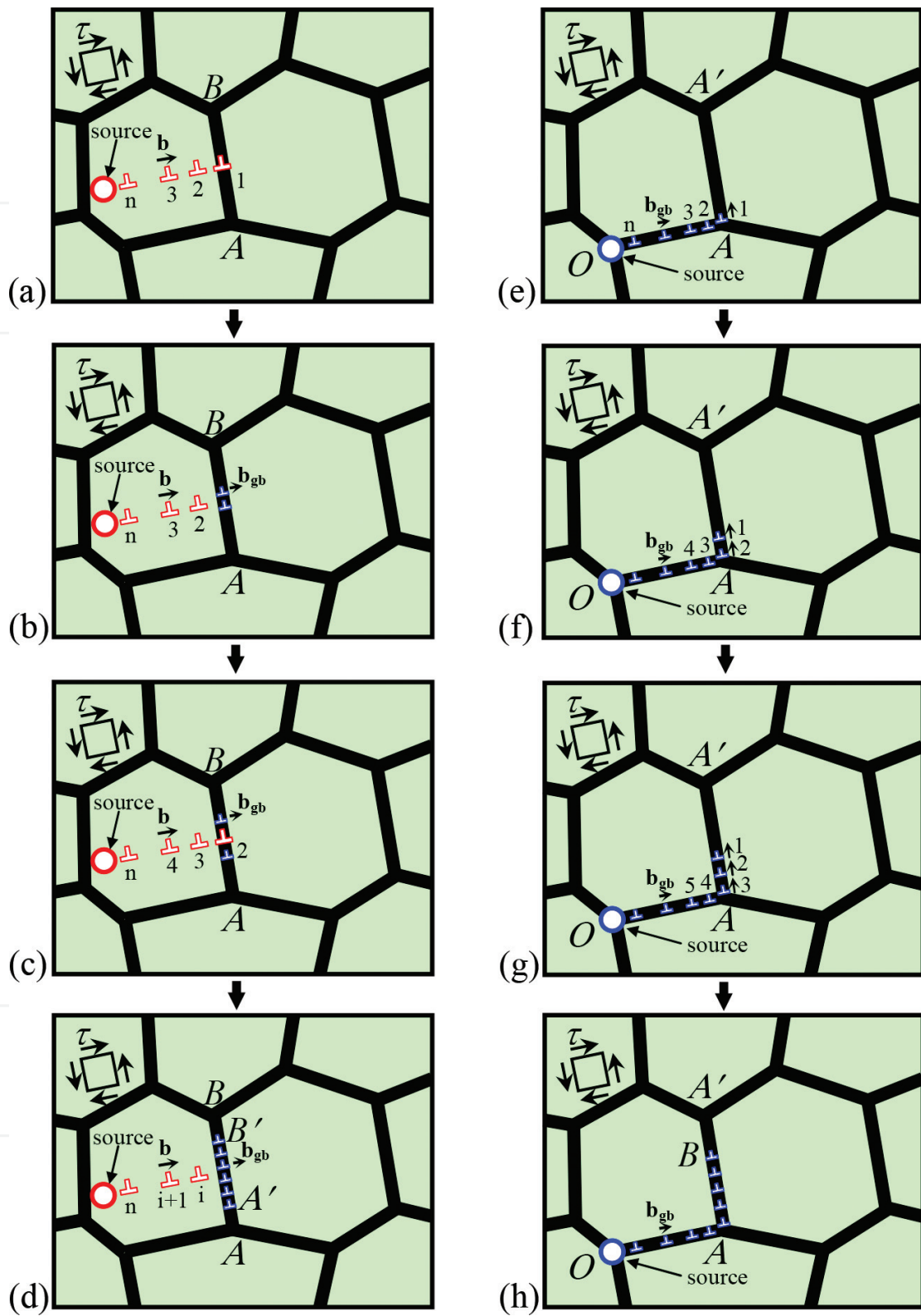


Figure 1. Mechanisms of formation of locally distorted GBs (grain boundaries) in nanocrystalline specimen under mechanical load (schematically). (a)–(d) Formation of a nano-sized wall of extra GB dislocation $A'B'$ through successive splitting of the head dislocations belonging to the pile-up of lattice edge dislocations stopped by GB AB and climb process of GB dislocations along the GB AB . (e)–(h) Formation of a nano-sized wall of extra GB dislocation AB through successive splitting of the head dislocations belonging to the pile-up of GB dislocations stopped by GB AA' and climb process of GB dislocations along the GB AA' .

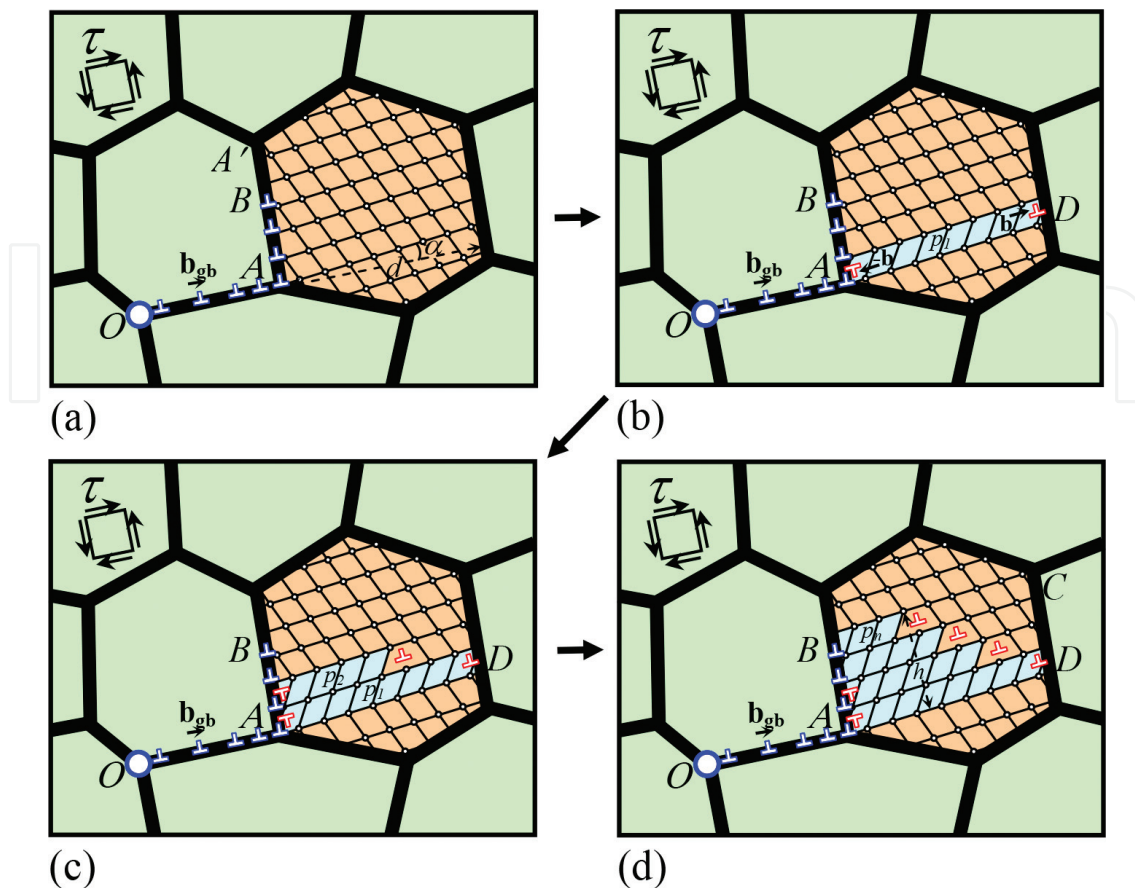


Figure 2. Mechanism of formation of nanoscale twins at locally distorted GBs (grain boundaries) through successive emission of partial dislocations in a nanocrystalline specimen under mechanical load (schematically). (a)–(d) Processes of successive dislocation emission from locally distorted GB fragment *AB* that move in adjacent grain interior and form a nanoscale twin *ABCD*.

fabricated by severe plastic deformation methods, and they can contain nanoscale fragments with GB dislocations located on every slip plane.

Thus, micromechanisms of nanotwin formation at locally distorted GB segments represent: (1) the consequent emission of partial dislocations from GBs; (2) the cooperative emission of partial dislocations from GBs; and (3) the generation of multiphase nanoscale shear at GBs. The former two micromechanisms of nanoscale twins generation occur through splitting of the GB dislocations into immobile GB dislocations and mobile partial dislocations (**Figures 2 and 3**). Consequent (**Figure 2**) or cooperative (**Figure 3**) gliding of the mobile dislocations along neighboring slip planes in a grain interior results in formation of a nanotwin.

Note that an energy barrier specifying the transformation of a GB dislocation at a local distorted GB segment into another GB dislocation and a partial dislocation (**Figures 2 and 3**) is around the energy of a partial dislocation. Thus, this barrier is lower than the barrier required for multiplication of partial dislocations (being around the energy of a full dislocation) considered by Zhu and coworkers [13]. In these circumstances, the splitting transformation (**Figures 2 and 3**) is more energetically favored as compared to the multiplication reaction.

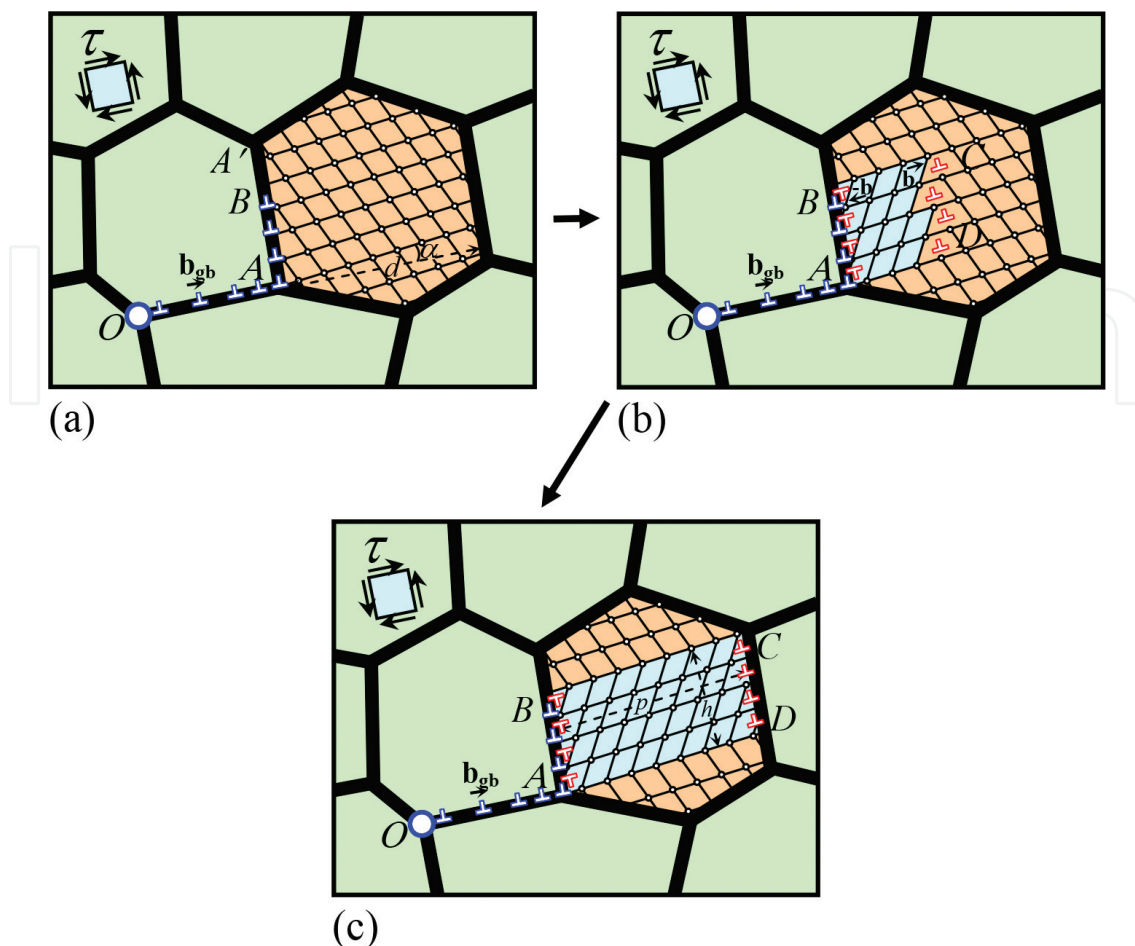


Figure 3. Mechanism of formation of nanoscale twins at locally distorted GBs (grain boundaries) through cooperative emission of partial dislocations in a nanocrystalline specimen under mechanical load (schematically). (a)–(c) Partial dislocation cooperatively emit from locally distorted GB fragment AB and move in adjacent grain interior toward the opposite GB forming a nanoscale twin ABCD.

The third mechanism for nanotwin formation at a locally distorted GB is multiplane nanoscale shear (**Figure 4**) firstly defined in Letter [19]. Following [19], a multiplane nanoscale shear is an ideal (rigid body) shear occurring simultaneously along several neighboring crystallographic planes within a nanoscale region—a three-dimensional region having two or three nanoscopic sizes—in a crystalline solid (this notion is based on that of multiplane ideal shear in infinite crystals [20]). The multiplane shear is characterized by the shear magnitude s (which is identical at any time moment, for all the planes where the shear occurs) gradually growing from 0 to the partial dislocation and geometric sizes of the nanoscale region where the shear occurs. For certain value of s , a nanotwin is generated within the region in question (**Figure 4**). Let us discuss in more detail geometric and energetic characteristics of the three mechanisms for nanotwin formation at locally distorted GBs.

2.1. Nanotwin formation due to consequent emission of partial dislocations

Figure 2 illustrates geometric features of nanotwin formation at locally nonequilibrium GBs in nanomaterials in the situation where local GB fragments with extra GB dislocations are formed

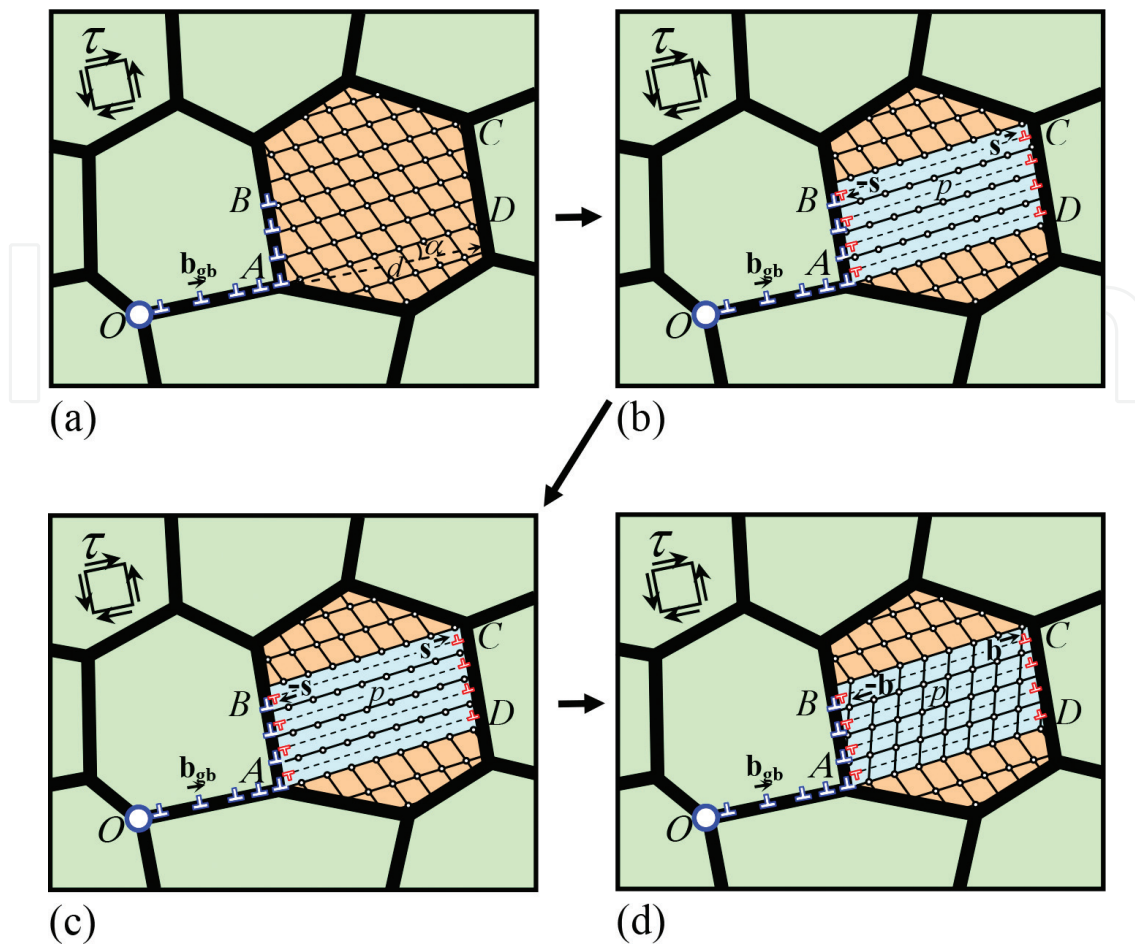


Figure 4. Mechanism of formation of nanoscale twins at locally distorted GBs (grain boundaries) through nanoscale multiplane shear in a nanocrystalline specimen under mechanical load (schematically). (a)–(d) Generation of nanotwin ABCD through subsequent transformation of non-crystallographic dislocations with Burgers vectors $\pm s$ into twinning partial dislocations.

due to both GB sliding and stress-driven climb of GB dislocations. As a result, a nanoscale wall configuration AB of GB dislocations is formed at GB AA' (**Figure 2a**). In the framework of the model, the GB dislocations forming the wall of climbing dislocations transform into immobile GB dislocations (staying at the GB AA') and mobile partial dislocation which are emitted from the GB AA' and can move along neighboring slip planes {111} in an adjacent grain (**Figure 2b–d**). In terms of the continuum approach, the emission of partial dislocations can be represented as formation of dislocation dipoles with Burgers vectors $\pm b$ and stacking faults (**Figure 2b–d**). Consequent generation of such dipoles of partial dislocations joined by stacking faults is capable of forming a nanoscale twin (**Figure 2b–d**). Such consequent events of partial dislocation emission from GBs were examined in several theoretical works (see, e.g., [16, 17]), which, however, did not concern formation of locally nonequilibrium GB structures considered here as initial ones for nanotwin generation.

The angle α specifies orientation of {111} slip planes for partial dislocations relative to the GB AA' plane (**Figure 2a**). The magnitude of Burgers vectors of partial dislocations is equal to $b = a/\sqrt{6}$. The distance δ is between the neighboring slip planes {111} and is related to the

crystal lattice parameter a as follows $\delta = a/\sqrt{3}$. When the i th dislocation moves in the grain interior (**Figure 2b–d**), a stacking fault of the length p_i is formed behind it. The stacking fault is characterized by the specific energy (per its unit area) γ , which serves as a hampering force for the partial dislocation slip. The dislocation slip is driven by the shear stress τ . The first partial dislocation is emitted from the triple junction A (**Figure 2b**) and moves across the grain interior toward the opposite GB (**Figure 2b**) when the shear stress reaches its critical value of τ_{c1} . After emission, the first partial dislocation moves toward opposite GB and, depending on shear stress level τ , reaches the opposite GB or stops in the grain interior moving over some distance p_1 and creates the stress fields hampering emission of a new dislocation. The first emitted partial dislocation creates stress fields which hamper the emission of the second partial dislocation. As a corollary, the second partial dislocation may be emitted only if the external shear stress τ increases up to a new critical value $\tau_{c2} > \tau_{c1}$. More than that, the second dislocation under the shear stress τ_{c2} does not reach the opposite GB, but moves over some distance p_2 shorter than the distance p_1 moved by the first dislocation (**Figure 2c**). It is because the stress field created by the first dislocation hampers slip of the second partial dislocation.

Also, the discussed trends come into play during emission of other partial dislocations due to the effects of previously emitted dislocations. That is, the critical stress for emission of the n th dislocation is larger than that for emission of the $(n - 1)$ th dislocation ($\tau_{c(n)} > \tau_{c(n-1)}$), and this stress drives slip of the n th dislocation over the distance shorter than that moved by the $(n - 1)$ th dislocation ($p_n < p_{n-1}$) (**Figure 2**). As a result, the nanotwin has a shape schematically presented in **Figure 2d**. Nanotwins of such a shape have been experimentally observed in nanomaterials [13] (**Figure 5**).

To analyze the suggested model, we consider the energy characteristics of the nanoscale twin generation due to consequent emission of partial dislocations from locally nonequilibrium GBs (**Figure 2**). First, define the conditions which are necessary for the energetically favorable emission of the first partial dislocation, which can be represented as formation of a dipole AD of partial dislocations with Burgers vectors $\pm b$ (**Figure 2b**). Generation of this partial dislocation dipole is characterized by the energy change ΔW_1 (per unit length of the pile-up head dislocation) defined as $\Delta W_1 = \Delta W_{1,final} - W_{1,initial}$, where $W_{1,final}$ and $W_{1,initial}$ are the energies of the considered defect configuration in its final (**Figure 2b**) and initial (**Figure 2a**)

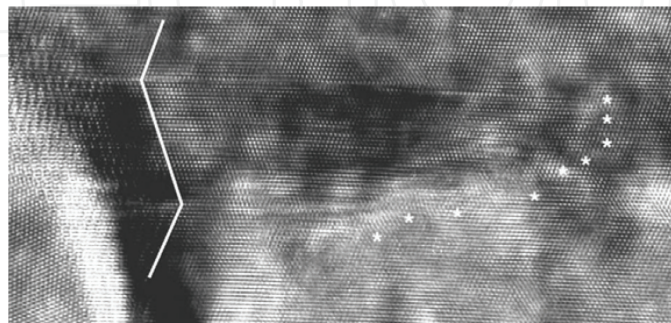


Figure 5. High resolution electron transmission microscopy image showing a deformation twin which ends in the grain interior as marked by the white asterisks in electrodeposited nanocrystalline Ni. Reprinted with permission from Ref. [13]. Copyright (2009), AIP Publishing LLC.

states, respectively. Formation of the dislocation dipole (**Figure 2b**) occurs as an energetically favorable process, if $\Delta W_1 < 0$. The energy change in question has the five terms:

$$\Delta W_1 = E^b + E^{\Delta-b} + E^{b-b_{gb}} + E_{\tau 1} + E_{\gamma 1}, \quad (1)$$

where E^b is the proper energy of the dipole of the Shockley partial dislocations having Burgers vectors $\pm b$; $E^{\Delta-b}$ is the energy that specifies the interaction between the partial dislocation dipole and the wall *AB* of GB dislocations; $E^{b-b_{gb}}$ is the energy that specifies the interaction between the partial dislocation dipole and the pile-up *OA* of GB dislocations; $E_{\tau 1}$ is the work spent by the external shear stress τ on movement of a mobile partial dislocation over the distance p ; and $E_{\gamma 1}$ is the energy of the stacking fault formed between the partial dislocations belonging to the dipole *AD*.

Detailed description of all the terms figuring on the right-hand side of Eq. (1) is given in the theoretical paper [14, 15]. Using Eq. (1), we calculated the dependences of the energy change ΔW_1 on the distance p_1 . We performed calculations for nanocrystalline nickel (Ni) and copper (Cu) for the following model parameter values characterizing Ni: $G = 73$ GPa, $\nu = 0.34$, $a = 0.352$ nm, $b_{gb} \approx 0.1$ nm, and $\gamma_{Ni} = 0.110$ J/m² [21] and Cu: $G = 44$ GPa, $\nu = 0.3$, $a = 0.358$ nm, $b_{gb} \approx 0.1$ nm, and $\gamma_{Cu} = 0.045$ J/m² [21]. The dependences $\Delta W_1(p_1)$ were calculated, for $d = 30$ nm, $n_c = 5$, $\tau = 100$ MPa and various values of α . The dependences $\Delta W_1(p_1)$ show the trend that emission of the first dislocation is enhanced when α decreases, and it is the most favorable at $\alpha = 0^\circ$.

Now let us consider the energy characteristics of emission of the n th partial dislocation, for $n > 1$. Emission of the n th partial dislocation is equivalent to formation of the n th dislocation dipole (**Figure 2**) in the nanocrystalline solid initially containing the dislocation-pile up and $(n - 1)$ dipoles of partial dislocations is characterized by the energy change ΔW_n (per unit length of a partial dislocation) defined as $\Delta W_n = W_n - W_{n-1}$, where W_n and W_{n-1} are the energies of the considered defect configuration with n and $n - 1$ partial dislocation dipoles, respectively. Formation of the n th dislocation dipole (**Figure 2**) occurs as an energetically favorable process, if $\Delta W_n < 0$. The energy change ΔW_n can be represented as follows:

$$\Delta W_n = E_{\Sigma}^{b(n)} - E_{\Sigma}^{b(n-1)} + E_{\Sigma}^{c-b(n)} - E_{\Sigma}^{c-b(n-1)} + E_{\Sigma}^{\Delta-b(n)} - E_{\Sigma}^{\Delta-b(n-1)} + E_{\Sigma}^{b-b(n)} - E_{\Sigma}^{b-b(n-1)} + E_{\gamma\Sigma}^{(n)} - E_{\gamma\Sigma}^{(n-1)} + E_{\tau\Sigma}^{(n)} - E_{\tau\Sigma}^{(n-1)}, \quad (2)$$

where $E_{\Sigma}^{b(n-1)}$ and $E_{\Sigma}^{b(n)}$ are the total self-energies of $(n - 1)$ and n partial dislocation dipoles, respectively; $E_{\Sigma}^{\Delta-b(n-1)}$ is the elastic interaction energy of $(n - 1)$ partial dislocation dipoles with the wall *AB* of GB dislocations; $E_{\Sigma}^{\Delta-b(n)}$ is the elastic interaction energy of n partial dislocation dipoles with the wall *AB* of GB dislocations; $E_{\Sigma}^{c-b(n-1)}$ and $E_{\Sigma}^{c-b(n)}$ are the elastic interaction energies of the GB dislocation pile-up *OA* with $(n - 1)$ and n partial dislocation dipoles, respectively; $E_{\Sigma}^{b-b(n-1)}$ and $E_{\Sigma}^{b-b(n)}$ are the sums of the energies specifying the dipole-dipole interaction in situations with $n - 1$ and n dislocation dipoles, respectively; $E_{\gamma\Sigma}^{(n-1)}$ and

$E_{\gamma\Sigma}^{(n)}$ are the sums of the energies specifying the stacking faults in situations with $(n - 1)$ and n dislocation dipoles, respectively; $E_{\tau\Sigma}^{(n-1)}$ and $E_{\tau\Sigma}^{(n)}$ are the sums of the energies specifying the interaction between the external shear stress τ as well as $(n - 1)$ and n partial dislocation dipoles, respectively. Detailed description of all the terms figuring on the right-hand side of Eq. (2) is given in the theoretical papers [14, 15]. With the help of Eq. (2) for the energy change ΔW_n , we calculated dependences of ΔW_n on the distance p_n . With these dependences, we also calculated the critical shear stress $\tau_{c(n)}$ (that can be defined as the minimum stress at which emission of the n th partial dislocation from the GB occurs). The critical stress $\tau_{c(n)}$ is calculated from the equation $\Delta W_n(p_n = 1\text{nm}) = 0$. The dependences of critical shear stress $\tau_{c(n)}$ on nanotwin thickness are presented in **Figure 6**. As it follows from the dependences $\tau_{c(n)}(h)$, the critical shear stress $\tau_{c(n)}$ decreases when the grain size d increases and/or the nanotwin thickness h decreases. For instance, for $d = 50$ nm, the generation of a nanotwin having the thickness $h = 3$ nm occurs in Cu at the critical shear stress $\tau_{c(n)} \approx 2.2$ GPa (**Figure 6**). This value is very high, but it can be reached in shock load tests of nanocrystalline materials.

2.2. Nanotwin formation due to cooperative emission of partial dislocations

The second micromechanism of nanotwin formation is realized through cooperative emission of partial dislocations from locally distorted GBs in deformed nanomaterials. As in the previous case, the initial defect configuration represents a nanoscale wall of GB dislocations AB located on every (or almost every) slip plane (**Figure 3a**). In this situation, the GB dislocations cooperatively emit from GB and move together along neighboring slip plane forming a nanotwin (**Figure 3b** and **c**). This mechanism in the situation where the GB dislocations are located on every slip plane has been considered in theoretical papers [14, 15]. As a result, the nanotwin $ABCD$ crosses the grain and joins two opposite GBs (**Figure 3c**). Such nanotwins have been experimentally observed in nanocrystalline nickel (Ni) [11] (**Figure 7**).

However, cooperative emission of partial dislocations from GBs also can occur in situation where the GB dislocations in the initial wall configuration AB are located on not all of slip planes. In this case, there are some gaps in arrangement of the GB b_{gb} -dislocations at GB fragment AB . Transformations of the GB b_{gb} -dislocations can occur in only a part of the set of

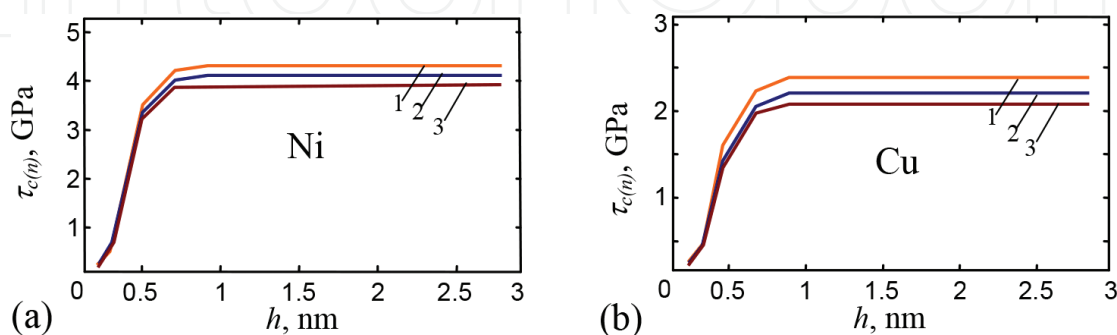


Figure 6. Dependences of the critical shear stress $\tau_{c(n)}$ on the nanotwin thickness h in the exemplary cases of nanocrystalline (a) nickel (Ni) and (b) copper (Cu), for various values of grain size $d = 25$ (curve 1), 50 (curve 2) and 100 (curve 3) nm.

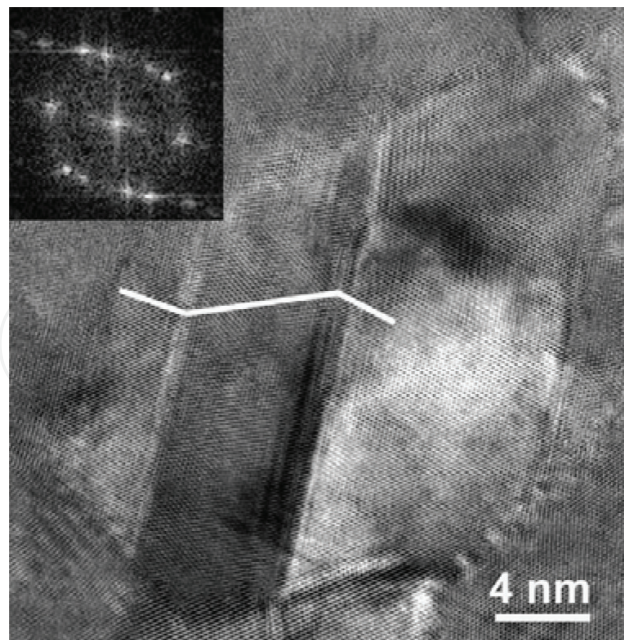


Figure 7. High resolution electron transmission microscopy image showing a deformation twin which crosses the grain interior and joins two opposite grain boundaries in nanocrystalline Ni. Reprinted from Ref. [11]. Copyright (2008), with permission from Elsevier.

crystallographic {111} planes adjacent to the GB fragment *AB* (**Figure 3**). Nevertheless, a nanotwin can be generated through cooperative emission of partial dislocations from such a GB fragment, if partial dislocations are generated on slip planes where the initial GB dislocations are absent.

Analyze the energy characteristics of the twin formation due to cooperative emission of dislocations from GB in nanomaterials (**Figure 3**). The cooperative emission process (**Figure 3**) is characterized by the energy difference $\Delta W'_n = W'_n - W'$, where W'_n and W' are the energies of the defect configuration in its final (**Figure 3b** and **c**) and initial (**Figure 3a**) states, respectively (after and before the emission process, respectively). In this situation, the nanotwin generation is energetically favorable, if $\Delta W'_n < 0$. The energy difference $\Delta W'_n$ has the six basic terms:

$$\Delta W'_n = E_{\Sigma n}^b + E_{\Sigma n}^{c-b} + E_{\Sigma n}^{\Delta-b} + E_{\Sigma n}^{b-b} + E_{\Sigma n}^{\gamma} + E_{\Sigma n'}^{\tau} \quad (3)$$

where $E_{\Sigma n}^b$ is the total self-energies of n partial dislocation dipoles; $E_{\Sigma n}^{\Delta-b}$ is the elastic interaction energy of n partial dislocation dipoles with the nanoscale wall *AB* of GB dislocations; $E_{\Sigma n}^{c-b}$ is the elastic interaction energy of the GB dislocation pile-up *OA* with n partial dislocation dipoles; $E_{\Sigma n}^{b-b}$ is the elastic energy of all the dipole-dipole interactions for n dislocation dipoles; E_n^{γ} is the energy of the twin boundaries; and $E_{\Sigma n'}^{\tau}$ is the elastic interaction energy of the external shear stress τ with n partial dislocation dipoles.

Calculation of all the terms figuring on the right-hand side of Eq. (3) is given in the theoretical paper [14, 15]. With the help of Eq. (3) for the energy change $\Delta W'_n$, we revealed dependences of

$\Delta W'_n$ on the distance p moved by the n partial dislocation in bulk of grain. With these results, we also calculated the critical shear stress $\tau'_{c(n)}$ that is the minimum stress at which the cooperative emission of n partial dislocation from GB is energetically favorable (**Figure 3**). More precisely, the critical shear stress $\tau'_{c(n)}$ can be found from the conditions that $\Delta W'_n(p = p') = 0$ (where $p' = 1\text{nm}$), $\Delta W'_n|_{p>p'} < 0$, and $\frac{\partial \Delta W'_n}{\partial p}|_{p>p'} \leq 0$.

Note that, if the inequalities $\Delta W'_n|_{p>p'} < 0$ and $\frac{\partial \Delta W'_n}{\partial p}|_{p>p'} < 0$ are valid, the dependences of the energy change $\Delta W'_n(p)$ on the distance p moved by the partial dislocation group within a grain are monotonously decreasing and negatively valued functions. In this case, the group AB of n partial b -dislocations is generated from locally distorted GB AA' and move across the grain over the distance $p = d$ toward the opposite GB where it is stopped. As a corollary, a nanotwin is formed which joins the two opposite GBs (**Figure 3c**).

In another case, the inequalities $\Delta W'_n|_{p>p'} < 0$, $\frac{\partial \Delta W'_n}{\partial p}|_{p=p_{eq}} = 0$ and $\frac{\partial^2 \Delta W'_n}{\partial p^2}|_{p=p_{eq}} > 0$ are valid. In this case, a function $\Delta W'_n(p)$ has its minimum corresponding to the equilibrium distance p_{eq} moved by the group of the emitted partial b -dislocations or, in other words, the equilibrium position p_{eq} of the nanotwin front AB of the nanotwin $ABCD$ (**Figure 3b**).

Dependences of the critical shear stress $\tau'_{c(n)}$ on the nanotwin thickness h , for various values of n_c , are presented in **Figure 8**. As it is seen in **Figure 8**, values of the critical shear stresses $\tau'_{c(n)}$ decrease with raising the number n_c of GB dislocations in the pile-up OA (see **Figure 3**).

2.3. Nanotwin formation due to generation of nanoscale multiplane shear

The third mechanism of nanotwin formation is realized through the generation of nanoscale multiplane shear at locally distorted GBs in deformed nanomaterials (**Figure 4**). As it has been noted previously, nanoscale multiplane shear is defined in work [19] as a multiplane ideal shear occurring within a nanoscale region, a three-dimensional region having two or three nanoscopic sizes. For instance, nanoscale multiplane shear can occur and produce a twin

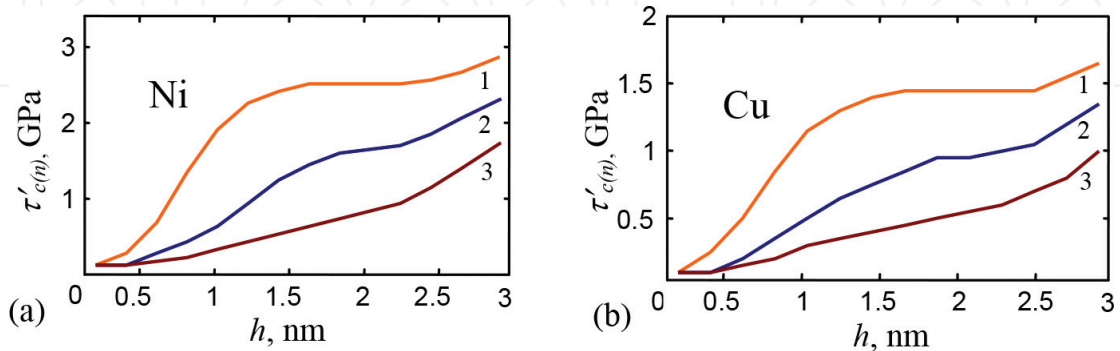


Figure 8. Dependences of the critical shear stress $\tau'_{c(n)}$ on the nanotwin thickness h in the exemplary cases of nanocrystalline (a) nickel (Ni) and (b) copper (Cu), for various values of grain boundary dislocations in the pile-up $n_c = 4$ (curve 1), 6 (curve 2) and 8 (curve 3).

within a nanoscale internal region of a grain of a deformed nanomaterial (**Figure 4**). More precisely, in the model situation, a deformation twin is produced under the action of a shear stress τ (**Figure 4**) through nanoscale multiplane shear or, in terms of the dislocation theory, through simultaneous nucleation of n dipoles of noncrystallographic dislocations with tiny Burgers vectors $\pm s$ (**Figure 4a–d**). The noncrystallographic dislocations of the dipoles are formed at opposite GB fragments, AB and CD , on adjacent $\{111\}$ planes. The Burgers vectors $\pm s$ of all the dislocations are the same in magnitude and grow simultaneously from zero to the Burgers vectors $\pm b$ of partial dislocations during the nanotwin formation process. In doing so, since there are preexistent GB dislocations at the GB fragment AB , the noncrystallographic dislocations at the GB fragment AB merge with these preexistent GB dislocations. As a corollary, during the nanotwin formation process, evolution of the noncrystallographic dislocations at the GB fragment AB manifests itself in evolution of the GB dislocations at this fragment (**Figure 4b–d**).

In the case of fcc metals (in particular, copper (Cu)), the generated dipoles of noncrystallographic partial dislocations are formed in adjacent slip planes $\{111\}$ assumed to be normal to the grain boundary fragments AB and CD . The region $ABCD$ (a rectangle with sizes h and p) is subjected to nanoscale multiplane shear, which leads to the formation of a nanoscale twin within this region (**Figure 4**). In doing so, AB length = CD length = h ; and AD length = BC length = p , where $p = d / \cos \alpha$ and d is the grain size (**Figure 4a**). As with the previously considered mechanisms for nanotwin formation, the distance δ between neighboring dipoles of Shockley dislocations is equal to the distance between the neighboring slip planes $\{111\}$ and is in the following relationship with the crystal lattice parameter a : $\delta = a / \sqrt{3}$.

Analyze energetic characteristics of the generation of nanoscale twins through nanoscale multiplane shear initiated at locally distorted GBs in nanocrystalline materials (**Figure 4**). In this case, in terms of the dislocation theory, a deformation twin is produced under the action of a shear stress τ through simultaneous nucleation of n dipoles of noncrystallographic dislocations with tiny Burgers vectors $\pm s$ whose magnitudes $n = 3$ gradually grow from 0 to b during the nanotwin formation process (**Figure 4**).

In general, the energy change ΔW_N that characterizes the nanotwin generation through multiplane nanoscale shear (**Figure 4**) has the seven key terms:

$$\Delta W_N = E_{\Sigma n}^s + E_{\Sigma n}^{c-s} + E_{\Sigma n}^{\Delta-s} + E_{\Sigma n}^{s-s} + W_{interior}(s) + W_{AC-BD}(s) + A, \quad (4)$$

Here $E_{\Sigma n}^s$ is the total self-energies of n dipoles of noncrystallographic $\pm s$ -dislocations; $E_{\Sigma n}^{c-s}$ is the elastic interaction energy of the pile-up of GB dislocations with n dipoles of noncrystallographic $\pm s$ -dislocations; $E_{\Sigma n}^{\Delta-s}$ is the elastic interaction energy of the wall AB of GB dislocations with n dipoles of noncrystallographic $\pm s$ -dislocations; $E_{\Sigma n}^{s-s}$ is the elastic energy of all dipole-dipole interactions for n dipoles of noncrystallographic $\pm s$ -dislocations; $W_{interior}$ denotes the energy of the interior area of the plastically sheared nanocrystal $ABCD$; W_{AD-BC} is the energy of the interfaces, AD and BC , between the sheared region $ABCD$ and the neighboring material; and A is the work of the external shear stress τ , spent to the plastic shear within the region $ABCD$.

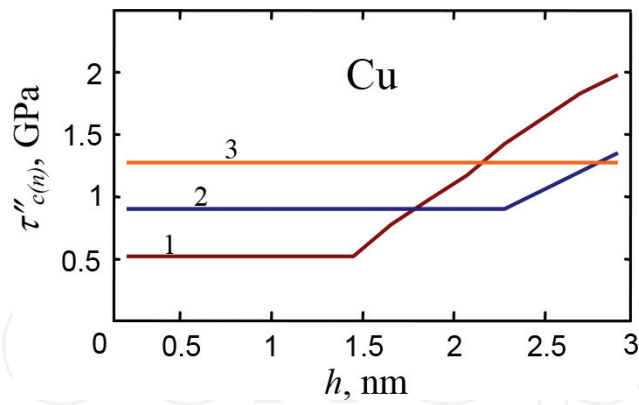


Figure 9. Dependences of the critical shear stress $\tau''_{c(n)}$ on the nanotwin thickness h in the exemplary cases of nanocrystalline copper (Cu), for various values of the grain size $d = 25$ (curve 1), 50 (curve 2) and 100 (curve 3) nm.

Calculations of all the terms figuring on the right-hand side of Eq. (4) are given in the theoretical paper [14, 15]. Based on these calculations in the exemplary cases of nanocrystalline Cu, we revealed dependences of the energy change ΔW_N on the Burgers vector magnitude s of the noncrystallographic dislocations for various sizes of the nanotwin. With functions $\Delta W_N(s)$, the critical shear stress $\tau''_{c(n)}$ (the minimum stress at which the nanotwin formation occurs) was calculated. As it follows from the dependences $\Delta W_N(s)$ the critical stress $\tau''_{c(3)} \approx 0.5$ GPa at $n = 3$, and $\tau''_{c(15)} \approx 2$ GPa at $n = 15$. The dependences of the critical shear stress $\tau''_{c(n)}$ on the nanotwin thickness h are presented in **Figure 9**, for various values of the grain size d . The dependences $\tau''_{c(n)}(h)$ show that the critical shear stress $\tau''_{c(n)}$ decreases when the grain size d increases and/or the nanotwin thickness h decreases (**Figure 9**).

3. Comparison of critical shear stress for nanotwin generation at grain boundaries due to various deformation mechanisms

In this section, we compare critical shear stresses for the considered mechanisms of nanotwin generation at locally distorted GBs in deformed nanomaterials. The dependences of the critical shear stresses $\tau_{c(n)}$ and $\tau'_{c(n)}$, for nickel (Ni), and $\tau_{c(n)}$, $\tau'_{c(n)}$ and $\tau''_{c(n)}$, for copper (Cu) on the nanotwin thickness h are presented in **Figure 10**. As it follows from **Figure 10**, for nickel (Ni), the cooperative emission of partial dislocations from GBs (**Figure 3**) is characterized by the lowest critical shear stress. In the case of Cu, the competition between different deformation mechanisms is more complicated. Therefore, for Cu, the mechanism of cooperative dislocation emission is realized at the lowest stress level $\tau'_{c(n)} < \tau''_{c(n)} < \tau_{c(n)}$ in the case of ultrathin nanotwin generation (with thickness $h < 1$ nm). At the same time, for Cu, the mechanism of nanoscale multiplane shear (**Figure 4**) occurs at the lowest stress level (**Figure 10**) in the range of nanotwin thickness h from 1 to 2 nm. For large nanotwins with thickness $h > 2$ nm, the mechanism of the cooperative emission of partial dislocations from GBs (**Figure 3**) is the most favorable process in copper again (**Figure 10**).

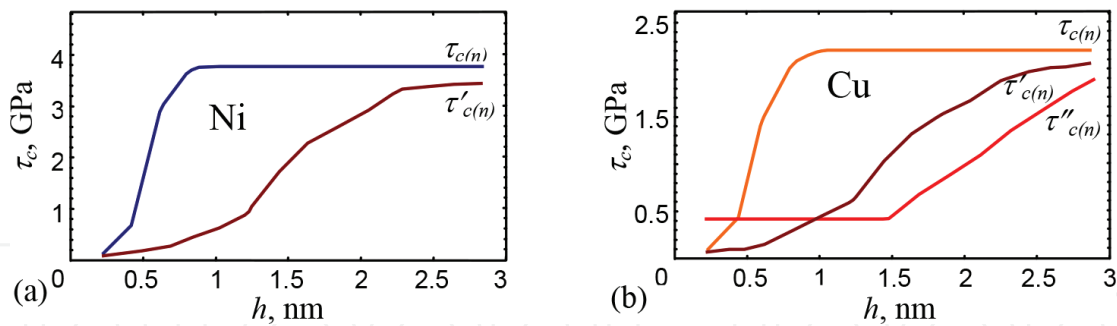


Figure 10. Dependences of the critical stresses $\tau_{c(n)}$ and $\tau'_{c(n)}$, for (a) nickel (Ni) and $\tau_{c(n)}$, $\tau'_{c(n)}$ and $\tau''_{c(n)}$, for (b) copper (Cu) on nanotwin thickness h .

According to results presented in **Figure 10**, the consequent emission of partial dislocations from locally distorted GBs is not favored. However, the critical stresses at which nanotwin generation mechanisms occur are highly sensitive to material parameters and the initial state of a locally distorted GB. Therefore, in the situations with other initial states and/or other materials, the consequent emission of partial dislocations from locally distorted GBs may be favored.

4. Conclusions

Thus, new specific micromechanisms of nanotwin generation at GBs in deformed nanocrystalline and ultrafine-grained materials were developed and analyzed. These micromechanisms describe the formation of deformation nanotwins at locally distorted GBs that contain segments being rich in GB dislocations produced by preceding plastic deformation. The micromechanisms of deformation twin formation occur through (1) the consequent emission of partial dislocations from GBs (**Figure 2**); (2) the cooperative emission of partial dislocations from GBs (**Figure 3**); and (3) the generation of multiplane nanoscale shear at GBs (**Figure 4**). It is found that the deformation twinning mechanisms (**Figures 2–4**) can operate in nanocrystalline and ultrafine-grained materials at rather high, but realistic levels of the stress (**Figures 6 and 8–10**). The suggested representations on generation of nanotwins at locally distorted GBs (see also [14, 15]) logically explain numerous experimental observations [11, 13] of generation of nanoscale twins at GBs in nanocrystalline and ultrafine-grained materials. These deformation twinning mechanisms illustrate complicated interactions between different deformation modes such as deformation twinning, GB sliding, and GB dislocation climb.

Acknowledgements

This work were supported by the Russian Fund of Basic Research (grant 16-32-60110) and Russian Ministry of Education and Science (task 16.3483.2017/PCh).

Author details

Nikolay Skiba^{1,2,3*}

*Address all correspondence to: nikolay.skiba@gmail.com

1 Institute for Problems of Mechanical Engineering, Russian Academy of Sciences, St. Petersburg, Russia

2 Research Laboratory for Mechanics of New Materials, Peter the Great St. Petersburg Polytechnic University, St. Petersburg, Russia

3 Department of Mathematics and Mechanics, St. Petersburg State University, St. Petersburg, Russia

References

- [1] Koch CC, Ovid'ko IA, Seal S, Veprek S. Structural Nanocrystalline Materials: Fundamentals and Applications. Cambridge: Cambridge University Press; 2007. 380 p. DOI: 10.1017/CBO9780511618840
- [2] Hahn H, Mondal P, Padmanabhan KA. A model for the deformation of nanocrystalline materials. *Philosophical Magazine B*. 1997;**76**(4):559-571. DOI: 10.1080/01418639708241122
- [3] Wang Y, Chen M, Zhou F, Ma E. High tensile ductility in a nanostructured materials. *Nature*. 2002;**419**(6910):912-915. DOI: 10.1038/nature01133
- [4] Ke M, Milligan WW, Hackney SA, Carsley JE, Aifantis EC. Observation and measurement of grain rotation and plastic strain in nanostructured metal thin films. *Nanostructured Materials*. 1995;**5**(6):689-697. DOI: 10.1016/0965-9773(95)00281-I
- [5] Feng H, Fang QH, Zhang LC, Liu YW. Special rotational deformation and grain size effect on fracture toughness of nanocrystalline materials. *International Journal of Plasticity*. 2013;**42**:50-64. DOI: 10.1016/j.ijplas.2012.09.015
- [6] Gutkin MY, Ovid'ko IA, Skiba NV. Crossover from grain boundary sliding to rotational deformation in nanocrystalline materials. *Acta Materialia*. 2003;**51**:4059-4071. DOI: 10.1016/S1359-6454(03)00226-X
- [7] Sansoz F, Dupont V. Quasicontinuum study of incipient plasticity under nanoscale contact in nanocrystalline aluminum. *Acta Materialia*. 2008;**56**:6013-6026. DOI: 10.1016/j.actamat.2008.08.014
- [8] Bobylev SV, Morozov NF, Ovid'ko IA. Cooperative grain boundary sliding and nanograin nucleation process in nanocrystalline, ultrafine-grained, and polycrystalline solids. *Physical Review B—Condensed Matter and Materials Physics*. 2011;**84**(9):094103. DOI: 10.1103/PhysRevB.84.094103

- [9] Ovid'ko IA, Skiba NV, Mukherjee AK. Nucleation of nanograins near cracks in nanocrystalline materials. *Scripta Materialia*. 2010;**62**:387-390. DOI: 10.1016/j.scriptamat.2009.11.035
- [10] Chen M, Ma E, Hemker KJ, Sheng H, Wang Y, Cheng X. Deformation twinning in nanocrystalline aluminum. *Science*. 2003;**300**:1275-1277. DOI: 10.1126/science.1083727
- [11] Wu X-L, Ma E. Dislocations and twins in nanocrystalline Ni after severe plastic deformation: The effects of grain size. *Materials Science and Engineering A*. 2008;**483-484**:84-86. DOI: 10.1016/j.msea.2006.07.173
- [12] Zhu YT, Liao XZ, Wu X-L. Deformation twinning in nanocrystalline materials. *Progress in Materials Science*. 2012;**57**:1-62. DOI: 10.1016/j.pmatsci.2011.05.001
- [13] Zhu YT, Wu X-L, Liao XZ, Narayan J, Mathaudhu SN, Kecskes LJ. Twinning partial multiplication at grain boundary in nanocrystalline fcc metals. *Applied Physics Letters*. 2009;**95**:031909. DOI: 10.1063/1.3187539
- [14] Ovid'ko IA, Skiba NV. Generation of nanoscale deformation twins at locally distorted grain boundaries in nanomaterials. *International Journal of Plasticity*. 2014;**62**:50-71. DOI: 10.1016/j.ijplas.2014.06.005
- [15] Ovid'ko IA, Skiba NV. Nanotwins induced by grain boundary deformation processes in nanomaterials. *Scripta Materialia*. 2014;**71**:33-36. DOI: 10.1016/j.scriptamat.2013.09.028
- [16] MYu G, Ovid'ko IA, Skiba NV. Generation of deformation twins in nanocrystalline metals: Theoretical model. *Physical Review B—Condensed Matter and Materials Physics*. 2006;**74**:172107. DOI: 10.1103/PhysRevB.74.172107
- [17] Gutkin MY, Ovid'ko IA, Skiba NV. Crack-stimulated generation of deformation twins in nanocrystalline metals and ceramics. *Philosophical Magazine*. 2008;**88**:1137-1151. DOI: 10.1080/14786430802070813
- [18] Lojkowski W, Fecht H. The structure of intercrystalline interfaces. *Progress in Materials Science*. 2000;**45**:339-568. DOI: 10.1016/S0079-6425(99)00008-0
- [19] Ovid'ko IA. Nanoscale multiplane shear and twin deformation in nanowires and nanocrystalline solids. *Applied Physics Letters*. 2011;**99**:061907. DOI: 10.1063/1.3620934
- [20] Boyer RD, Li J, Ogata S, Yip S. Analysis of shear deformations in Al and Cu: Empirical potentials versus density functional theory. *Modelling and Simulation in Materials Science and Engineering*. 2004;**12**:1017-1029. DOI: 10.1088/0965-0393/12/5/017
- [21] Kibey S, Liu JB, Johnson DD, Sehitoglu H. Predicting twinning stress in fcc metals: Linking twin-energy pathways to twin nucleation. *Acta Materialia*. 2007;**55**:6843-6851. DOI: 10.1016/j.actamat.2007.08.042

